NJC

Accepted Manuscript

This is an *Accepted Manuscript*, which has been through the Royal Society of Chemistry peer review process and has been accepted for publication.

Accepted Manuscripts are published online shortly after acceptance, before technical editing, formatting and proof reading. Using this free service, authors can make their results available to the community, in citable form, before we publish the edited article. We will replace this *Accepted Manuscript* with the edited and formatted *Advance Article* as soon as it is available.

You can find more information about *Accepted Manuscripts* in the Information for Authors.

Please note that technical editing may introduce minor changes to the text and/or graphics, which may alter content. The journal's standard Terms & Conditions and the Ethical guidelines still apply. In no event shall the Royal Society of Chemistry be held responsible for any errors or omissions in this *Accepted Manuscript* or any consequences arising from the use of any information it contains.

ROYAL SOCIETY OF CHEMISTRY

www.rsc.org/njc

Equilibrium, Kinetic and Thermodynamic Adsorption Studies of Organic Pollutants from aqueous solution onto CNTs/C@Fe/Chitosan Composites

Jie Ma[a], Yuan Zhuang[a], Fei Yu[a,b]*

[a] State Key Laboratory of Pollution Control and Resource Reuse, School of Environmental Science and Engineering, Tongji University, 1239 Siping Road, Shanghai 200092, P. R. of China. Tel: 86-21-6598 1831; E-mail: jma@tongji.edu.cn.

[b] College of chemistry and environmental engineering, Shanghai Institute of Technology, Shanghai 2001418, China. ; E-mail:fyu@vip.163.com

Abstract: The adsorption of organic pollutants, including dyes (methylene blue(MB) and methyl orange(MO)), antibiotics (tetracycline(TC)), and organic arsenical compound (roxarsone(ROX)) is carried out on a new kind of CNTs/C@Fe/CS nanocomposite. The effect of solution pH, contact time, and temperature on adsorption properties have been studied. The adsorption process follows the pseudo-second-order kinetic model very well, and equilibrium studies fit well with Langmuir, Freundlich, and Temkin adsorption isotherms. The maximum uptakes of MB, MO, TC and ROX on CNTs/C@Fe/CS are found to be 111.1, 500.0, 125.0, and 142.9 mg/g, respectively. Parameters calculated from thermodynamic indicate that the adsorption process is exothermic, spontaneous and favorable. The removal of organic pollutants is obviously dependent on pH values and temperature. These results suggest that CNTs/C@Fe/CS nanocomposite could be effectively used for the removal of organic contaminants from wastewaters.

Keywords: Adsorption; Organic Pollutants; Carbon nanotubes; Chitosan;

1. Introduction

Carbon nanotubes (CNTs) have been regarded as the excellent adsorbents to remove the numerous organic pollutants due to high specific surface area [1, 2]. However, CNTs may cause environmental pollution if they are not well separated from aqueous solution after water treatment. Contrasted with filtration and centrifugation, magnetic separation is regarded as a more efficacious way [3]. More important, the modification of CNT would improve the efficiency and selectivity of adsorption during the removal of organic contaminants.

However, the preparation ways of traditional magnetic CNTs are complex and environmentally unfriendly [4]. For example, strong acid has to be used to remove organic matters and metals to get

purified CNTs. Then, the purified CNTs are lack of functional groups and need the further modification by oxidation treatment. Moreover, the magnetic nanoparticles on the surface of CNTs is uncovered, which would result in their agglomeration when magnetic force occurrs. At last, the low-yield and uneconomic production process of traditional magnetic CNTs goes against their practical use.

Chitosan (CS) is a kind of polysaccharide which has been widely used as an important biopolymer [5]. The preparation of nanocomposite composed of CNT and biopolymer would improve better adsorption performance. Thus, the toxicity of CNTs could be reduced and also the disadvantage of less functional groups could be solved. Moreoever, the improvement of CNTs dispersity is benefit for adsorption [6]. Usually, CNTs and CS could be covalently grafted through oxidation [7]. Carson *et al.* [7] prepared CNTs/CS composite and utilized in tissue engineering. Qian *et al.* [8] prepared CNTs and CS into a composite film and applicated as biosensor.

Herein, magnetic CNTs/C@Fe/CS is prepared by a facile method [9]. And then, the adsorption of organic pollutants, including of dyes, antibiotics and organic arsenical compound, is carried out on CNTs/C@Fe/CS. The CNTs/C@Fe/CS shows good adsorption performance, moreover, the kinetics, equilibrium and mechanism are also investigated.

2. Experimental

2.1 Materials and characterization

All chemicals are bought from Sinopharm Chemical Reagent Co., Ltd (Shanghai, China) which are analytical pure without any further purification before used in the experiments. All solutions are prepared using deionized water.

For the preparation of CNTs/C@Fe, chemical vapor deposition method is used [10]. Ferrocene is selected as a catalyst. Ethanol is choosen as the source of carbon. The growth promoter is thiophene. Ar air flow is use as protected gas to prevent oxidation. The ethanol solution is introduced by a squirming pump and sprayed driven by Ar flow. Finally, the CNTs/C@Fe could be collected.

For the preparation of CNTs/C@Fe/CS, equal quality of CS and CNTs/C@Fe of 10 mg are dispersed in dilute acetic acid solution (100 mL, 5 wt %); then 0.6 g $NaHSO_3$ is added into the solution, following by the addtion of formaldehyde solution after the bubbles disappeared. After washing by distilled water through vacuum filtration, the product is put into NaOH solution at pH=10 followed by the addition of 10 mL epichlorohydrin. The solution is heated in water bath at

90 ℃ for 6 h. The CNTs/C@Fe/CS is put into 1mol/L HCl solution for 30 min, then washed and vacuum freeze dried.

CNTs/C@Fe/CS are analyzed using high-resolution transmission electron microscopy (HRTEM, JEOL 2100F, accelerating voltage of 200 kV, Japan) to study the microstructure and morphology. High-resolution thermogravimetric analysis (TGA) is tested by a TA Instruments Q600 SDT thermal analyser. A superconducting quantum interference device magnetometer (MPMS XL7, Quantum Design) is used to investigate the magnetization property of CNTs/C@Fe/CS. The surface functional groups are observed by FT-IR (NEXUS, 670).

2.2 Batch adsorption experiments

To investigate organic pollutant adsorption ability of CNTs/C@Fe/CS, batch experiments are operated. In 1 L deionized water, 200 mg organic pollutant is dissolved to obtain the stock solution (200 mg/L). Through dilution of the the stock solution, various working solutions. All the adsorption process are operated under solid to liquid ratio of 1 mg/mL in flasks shaken by a thermostatic shaker under 200 rpm at 25 ℃. The separation after adsorption is carried out by magnetic force in advance and then filtered through a 0.45 μm membrane. A UV-visible absorption-based approach with an ultraviolet spectrophotometer (Tianmei UV-2310(II)) is used to measure the concentrations of the solutions by measuring absorbance changes.

Initial concentrations are set from 1 mg/L to 200 mg/L to study the adsorption isotherm under pH=6. Four kinds of adsorption isotherms, Langmuir, Freundlich, Temkin and Dubinin-Radushkevich (D-R) isotherms, are used as showed in equations (1) to (5). In the Langmuir isotherm, there is an assumed monolayer on the homogenous surface of the adsorbent formed by the adsorbate without interaction between the adsorbent and the adsorbate. In the Freundlich model, it is assumed that the adsorption happens on a heterogeneous surface, moreover, it is also proposed that there are multilayer adsorption accompanied by interaction among the adsorbate molecules. For the Temkin model, it is based on electrostatic interaction between opposite electrical charges for the chemical adsorption. As to the D-R isotherm model, it does not assume a homogenous surface. Then, to value whether an adsorption process is favorable, R_L, which is an significant parameter called the separation factor or equilibrium parameter is applied as showed in equation (6). E_{DR}, which represents the mean free energy of adsorption, is exhibited in equation (7) [11].

$$\frac{C_e}{q_e} = \frac{1}{K_L} + (\frac{\alpha_L}{K_L})C_e \quad (1)$$

$$Inq_e = InK_F + \frac{1}{n} InC_e \quad (2)$$

$$q_e = B_T InC_e + B_T InK_F \quad (3)$$

$$Inq_e = Inq_m - \beta\varepsilon^2 \quad (4)$$

$$\varepsilon_e = RTIn(1 + \frac{1}{C_e}) \quad (5)$$

$$R_L = \frac{1}{1 + K_L C_0} \quad (6)$$

$$E_{DR} = \frac{1}{(2\beta)^{0.5}} \quad (7)$$

Where K_L(L/g) and a_L(L/mg) are constants from Langmuir model, among which a_L reflects the adsorption energy. The Langmuir model is an ideal model that assumes a perfect adsorbent surface and monolayer molecule adsorption. The maximum adsorption capacity of the adsorbent which is the equilibrium monolayer capacity or saturation capacity q_m is equal to K_L/a_L numerically; K_F, B_T, K_T are constants from Freundlich and Temkin models, while n is the Freundlich linearity index. As an empirical model, the Freundlich model is used widely in chemistry. T (K) is the absolute temperature and R (8.314 J/mol K) is the ideal gas constant, K_c is the equilibrium constant.

To study the kinetic of the adsorption, three typical kinetic models which are pseudo-first-order (in view of solid capacity) showed in (8), pseudo-second-order (on account of solid phase adsorption) showed in (9) and intra-particle diffusion model (base on the diffusion mechanism) showed in (10), are used and the correlation coefficient (R^2) is also calculated [12].

$$\ln(q_e - q_t) = \ln q_e - \frac{k_1}{2.303} t \quad (8)$$

$$\frac{t}{q_t} = \frac{1}{k_2 q_e^2} + \frac{t}{q_e} \quad (9)$$

$$q_t = k_{id} t^{0.5} + C \quad (10)$$

where q_e and q_t represent the quantity of organic pollutants adsorbed (mg/g) at equilibrium and t means time (h), respectively; k_1 denotes the rate constant in the pseudo-first-order kinetic model (t^{-1}) and k_2 denotes the rate constant (g/mg·h) in the pseudo second-order kinetic model; k_{id} (mg/g·$h^{0.5}$) is the intra-particle diffusion rate constant and C (mg/g) is the adsorption capacity.

Three thermodynamic parameters are commonly considered to characterize the adsorption process which are the standard enthalpy ($\triangle H^0$), standard free energy ($\triangle G^0$) and standard entropy ($\triangle S^0$). The values of $\triangle H^0$ and $\triangle S^0$ can be obtained from the following equations (11) to (13)[13]:

$$InK_L = \frac{\Delta S^0}{R} - \frac{\Delta H^0}{RT} \quad (11)$$

$$\Delta G^0 = -RTInK_L \quad (12)$$

$$Ink_2 = InA - \frac{E_a}{RT} \quad (13)$$

Where R is the universal gas constant (8.314 J/mol K), T (K) is the absolute solution temperature and K_L (L/mg) is the constant in Langmuir isotherm. k_2 (g/mg h) is the rate constant in the pseudo second-order kinetic model, E_a (kJ/mol) is the Arrhenius activation energy of adsorption and A is the Arrhenius factor. $-E_a/R$ could be obtained from the slope of the plot of k_2 against 1/T.

The adsorption capacity (mg/g) is calculated as equation (14).

$$q_t = (C_0 - C_t) \times \frac{V}{m} \quad (14)$$

where C_0 and C_t are the initial concentrations and concentrations after a period of time (mg/L); V is the initial solution volume (L); and m is the adsorbent dosage(g).

3. Results and discussion

3.1 Characterization of CNTs/C@Fe/CS

TEM images of CNTs/C@Fe/CS (CS content 50 wt%) are shown in Fig. 1, there are abundant iron nanoparticles distributed on the surface of nanotubes, which could provide the magnetic property of CNTs/C@Fe/CS. The tubes are connected by CS. The diameter of the CNTs is about 20 nm and the particle size of the C@Fe is estimated to ~10 nm. The carbon shells are formed by graphitic layers as shown in Fig.1d, it would protect Fe nanoparticles against oxidation and agglomeration. Data of thermal and magnetization analyzes are shown in Table 1. The CNTs/C@Fe/CS exhibites a tiny hysteresis loop that is expected to respond well to magnetic fields without any permanent magnetization [14], the saturation magnetization Ms is 8.0 emu/g[1], the well magnetic characters of CNTs/C@Fe/CS are benefit for its separation after adsorption.

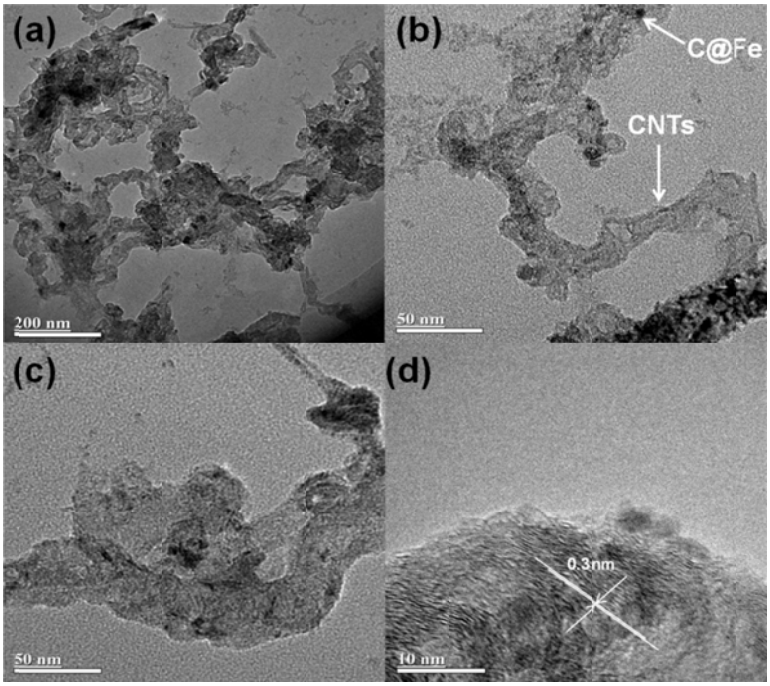

Fig. 1 TEM images of CNTs/C@Fe/CS.

Table 1 Physical and chemical properties of CNTs/C@Fe/CS.

CNTs (wt %)	Fe (wt %)	*Ms* (emu/g)	Coercive force(Oe)
95.4	4.6	8.0	16

3.2 Influence of CS content on adsorption

Nanoparticles embedded biopolymer materials have excellent potential adsorption application. Specially, the introduction of nanoparticles provides more active sites for adsorption [15]. Adsorption capacities of MB, MO, TC, and ROX with different CS contents are shown in Fig. 2. CNTs/C@Fe/CS shows excellent adsorption ability for the four pollutants under higher CS content. The adsorption capacities apparently increase with the increase of CS content especially while the CS content is below 50%. As CS adopts a positive surface charge which favors adsorption of anionic adsorbates, the MO adsorption has an obviously increase with the increasing CS content while the MB adsorption increases slowly. Moreover, the presence of the arsenate group increases the sorptive uptake of ROX due to the negative charged arsenate groups [16].

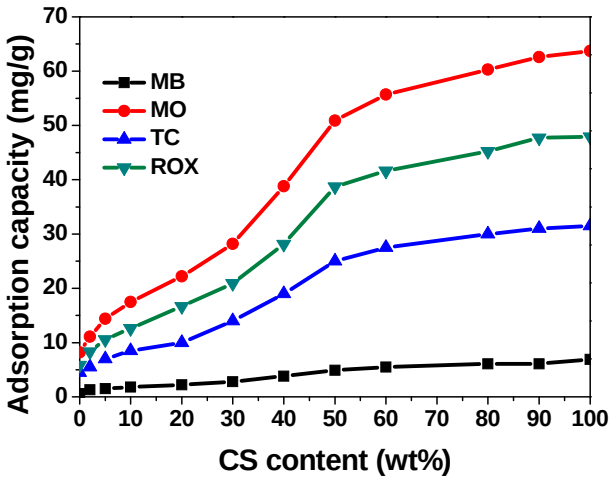

Fig. 2 Adsorption capacity of MB, MO, TC, and ROX on CNTs/C@Fe/CS with different CS contents.

3.3 Adsorption isotherms

To investigate adsorption mechanism, adsorption isotherm is necessary to be discussed. Adsorption isotherms of the four pollutants on CNTs/C@Fe/CS with 50 wt % CS are shown in Fig. 3. Parameters obtained from these four models are listed in Table 2. The maximum uptakes of MB, MO, TC and ROX on CNTs/C@Fe/CS are found to be 111.1, 500.0, 125.0, and 142.9 mg/g, respectively, which is better than previous reports, as shown in Table S1. The value of R_L is referred as an equilibrium parameter which could reflect whether the adsorption is unfavorable ($R_L > 1$), linear ($R_L = 1$), favorable ($0 < R_L < 1$) or irreversible ($R_L = 0$)[17]. In this study, the values of R_L are found to be less than 1 for all the four pollutants which indicate the adsorption processes are favorable for the four pollutants adsorption in this study. The applicability of Freundlich isotherm suggests that the intermolecular interactions exist between the pollutants and the adsorbent. To confirm the interaction between CNTs/C@Fe/CS and the pollutants, FT-IR tests of CNTs/C@Fe/CS before and after adsorption are shown in Fig. 3d. Peaks around 1562 cm^{-1} are assigned to the N–H bending of $–NH_2$ groups in CS [18]. The peaks around 3400 cm^{-1} comfirm the formation of -OH after adsorption for all the four pollutants [19]. The good coefficient with Temkin model indicates the heat of adsorption of all the four organic molecules in the layer would decrease linearly with coverage due to adsorbent–adsorbate interaction and the adsorption is drived by a uniform existence of binding energies [13]. Through D-R model, the mean adsorption energy (E) gives information about physical and chemical adsorption [20]. However, the data did not follow D-R isotherm model very well.

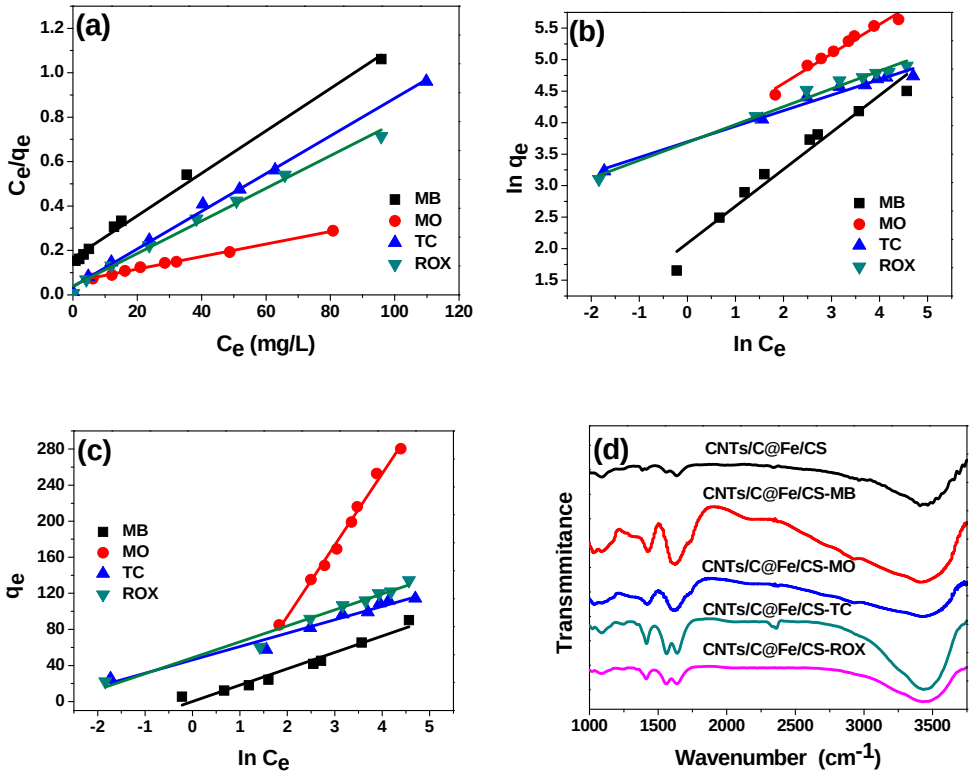

Fig. 3 Langmuir (a), Freundlich(b) and Temkin (c) adsorption isotherms model of MB, MO, TC and ROX on CNTs/C@Fe/CS; FT-IR spectra (d) of CNTs/C@Fe/CS before and after adsorption.

Table 2 The parameters derived from the Langmuir, Freundlich, Temkin, and D-R models.

Isotherm model	Parameters	MB	MO	TC	ROX
Langmuir	q_m(mg/g)	111.1	500.0	125.0	142.9
	q_m(mmol/g)	0.3	1.5	0.3	0.5
	K_L(L/mg)	6.1	16.9	27.0	25.6
	R_L	1.6×10^{-3}	5.9×10^{-4}	3.7×10^{-4}	3.9×10^{-4}
	R^2	0.993	0.997	0.996	0.991
Freundlich	K_F (L/g)	8.0	14.7	40.3	39.9
	n	1.7	2.1	4.0	3.5
	R^2	0.956	0.965	0.978	0.981
Temkin	K_T (L/mol)	18.1	79.2	14.9	17.7
	B_T	0.25	13.8	10.0	10.5
	R^2	0.957	0.990	0.963	0.971
D-R	R^2	0.662	0.769	0.785	0.811

3.4 Adsorption Kinetics

We use the pseudo-first-order, the pseudo-second-order, and the intra-particle diffusion model to investigate kinetics of the adsorption, as shown in Fig. 4. In Table 3, it can be seen that the linear plots of the pseudo-second-order models have the highest correlation coefficients(R^2) than the other three models in all the four pollutants. Thus, this process is more likely to predict the behavior over the whole procedure of adsorption. The linear plots of *t*/*qt* versus t show good consistency between the experimental and the calculated q_e values. Besides, the correlation coefficients for the second-order kinetic model are greater than 0.990 for all the four pollutants, indicating the feasibility of the second-order kinetic model to describe these adsorption processes. The intraparticle diffusion model is assumed to identify the adsorption mechanism and to forecast the rate controlling step, in this model, C is the intercept and k_{id} ($mg/g \cdot min^{0.5}$) is the intraparticle diffusion rate constant. There are three stages in the intraparticle diffusion model. The first stage is the external surface adsorption, while the second stage is the gradual stage of adsorption. While the plot of q_t versus $t^{0.5}$ is linear and passes through the origin, indicating the intraparticle diffusion is rate-controlled. The final stage is due to the low concentration of pollutants and the lack of available sorption sites [22]. In these adsorption processes, though the q_t and $t^{0.5}$ is linear, and the plot does not pass through the origin, indicating the processes are not rate-controlled [23]. These results suggest that it is proper to employ pseudo-second order kinetic model to express these adsorption processes. Therefore, mass transfer solution is not the rate-controlling step, and interactions between dye anions and CNTs/C@Fe/CS are involved in the adsorption mechanism [24, 25].

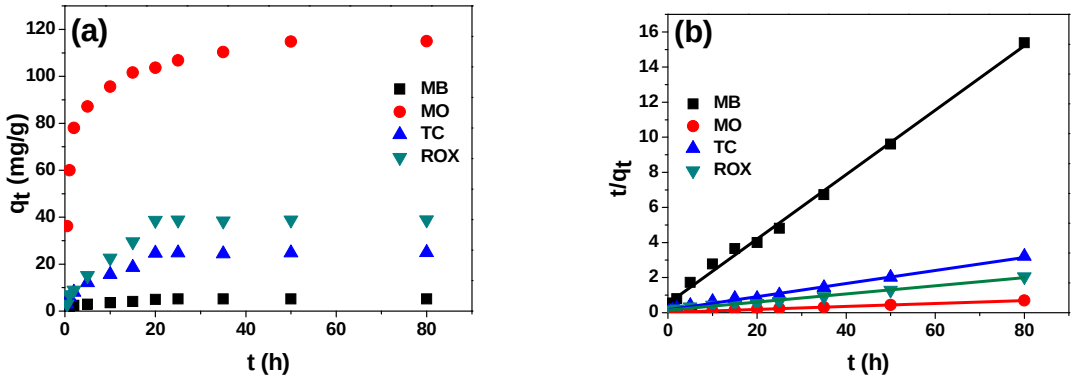

Fig. 4 Kinetic curves(a), pseudo-second order model(b).

Table 3 Kinetic parameters of pseudo first-order, second-order and intra-particle diffusion model.

Kinetic model	Parameters	MB	MO	TC	ROX
pseudo-first order	R^2	0.513	0.884	0.529	0.536

pseudo-second order	q_e(mg/g)	117.6	26.8	43.3	5.4
	k_2(min^{-1})	200.7	118.5	271.2	15.6
	R^2	0.999	0.994	0.999	0.996
Intra-particle diffusion	R^2	0.779	0.699	0.783	0.784

3.5 Adsorption thermodynamics

The calculated values of $\triangle H^0$, $\triangle S^0$, $\triangle G^0$, and E_a for adsorption are reported in Table 4. $\triangle H^0$ has positive values indicating that the adsorption processes are endothermic. It accords with the results that the adsorption capacities increase with increasing temperature[13]. The positive value of $\triangle S^0$ reflects good affinity of the CNTs/C@Fe/CS for the pollutants and the increasing randomness [26, 27]. $\triangle G^0$ have a negative value indicating the adsorption process is feasible and the adsorption is spontaneous. Moreover, the values of $\triangle G^0$ are found to decrease with increasing temperature casing by less driving force [17]. Meanwhile, the adsorption capability increases with the experimental temperature increasing. It is because under the higher temperature, the organic molecule could overcome space obstruction while diffusing into CNTs/C@Fe/CS [28].

Table 4 Thermodynamic parameters of MB, MO, TC and ROX adsorption on CNTs/C@Fe/CS.

Parameters	MB	MO	TC	ROX
△H◦(kJ/mol)	26864	44275	25240	27037
⊿*S*◦(kJ/mol)	105	171	111	117
⊿*G*◦(kJ/mol)(15 ℃)	-3492	-4979	-6920	-6638
⊿*G*◦(kJ/mol)(25 ℃)	-4464	-7012	-8168	-8037
⊿*G*◦(kJ/mol)(45 ℃)	-6118	-9288	-9726	-9586

3.6 Influence of pH on adsorption

The effects of pH on adsorption are illustrated in Fig. 5. The pH can have influence on adsorption through impact on the adsorbent surface charge, the ionization degree of pollutants, the functional groups dissociation on the adsorbent active sites and the structure of some pollutants. Apparently, both the adsorption capacities of MB and MO increased rapidly when solution pH is below 3 and then decreased at higher pH. The amino (–NH_2) and hydroxyl (–OH) groups in CS could provide active sites. CS surface is positively charged under acidic solutions [29]. The decrease of dye adsorption under higher pH may be resulted from the electrostatic interaction between

CNTs/C@Fe/CS and the dye anions. Under alkaline solution, the large amount of OH^- ions could compete with the dye anions [30-33]. As CNTs/C@Fe/CS has visibly higher adsorption capacities for MO than MB which is in accordance with other CS-based magnetic materials [28, 34], indicating it has better adsorption performance for negatively charged pollutants. This may suggest that at low pH, free amino groups in CS are protonated which could be benefit for the attraction of anionic dye [35]. For TC and ROX, CNTs/C@Fe/CS had higher adsorption abilities in higher pH. Undergoing protonation-deprotonation reactions, TC could present different charge species relying on pH. TC could be positive (pH < 3.3), neutral (3.3< pH< 7.68), one negative (7.68 < pH< 9.68) or two negative (pH > 9.68) [36], and ROX species are neutral (pH < 3.49), one negative (3.49< pH< 5.74), two negative (5.74< pH< 9.13)or three negative (pH > 9.13)[16]. The increase of TC and ROX adsorption under higher pH further reflects that CNTs/C@Fe/CS possesses better adsorption performance for negatively charged pollutants. Thus, besides physical adsorption, electrostatic interaction is also important in the organic pollutants adsorption on CNTs/C@Fe/CS.

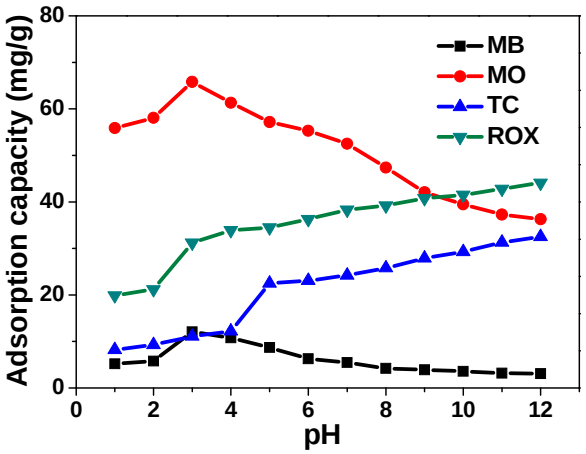

Fig. 5 Influence of pH values on MB, MO, TC and ROX adsorption on CNTs/C@Fe/CS.

4. Conclusions

In present study, adsorption properties of four organic pollutants on a novel CNTs/C@Fe/CS composite is investigated. The CNTs/C@Fe/CS showed to have better adsorption capacity for negatively charged pollutants. The equilibrium adsorption datas are well fitted by the Langmuir, Freundlich, and Temkin models. During kinetic study, the adsorption processes are found to fit the pseudo-second-order kinetic model better. Thermodynamic parameters $\triangle H^0$, $\triangle S^0$ and $\triangle G^0$ are also determined. $\triangle H^0$ has positive values indicating that the adsorption processes are

endothermic. The positive value of $\triangle S^0$ reflects good affinity of the CNTs/C@Fe/CS for the pollutants and the increasing randomness. $\triangle G^0$ have a negative value indicating the adsorption process is feasible and the adsorption is spontaneous. Thus, the resulting CNTs/C@Fe/CS has great potential for the removal of organic pollutants from aqueous solution.

Acknowledgements

This research is supported by the National Natural Science Foundation of China (No. 21207100)

References

1. F. Yu, J. H. Chen, M. X. Yang, L. Zhou, L. Jin, C. Su, F. L. Li, L. Chen, Z. W. Yuan, L. L. Yu and J. Ma, *New J Chem*, 2012, **36**, 1940-1943.

2. J. Ma, F. Yu, L. Zhou, L. Jin, M. X. Yang, J. S. Luan, Y. H. Tang, H. B. Fan, Z. W. Yuan and J. H. Chen, *Acs Appl Mater Inter*, 2012, **4**, 5749-5760.

3. F. Yu, J. H. Chen, L. Chen, J. Huai, W. Y. Gong, Z. W. Yuan, J. H. Wang and J. Ma, *J Colloid Interf Sci*, 2012, **378**, 175-183.

4. J. Ma, F. Yu, Z. Wen, M. Yang, H. Zhou, C. Li, L. Jin, L. Zhou, L. Chen, Z. Yuan and J. Chen, *Dalton transactions*, 2013, **42**, 1356-1359.

5. C. Lau, M. J. Cooney and P. Atanassov, *Langmuir*, 2008, **24**, 7004-7010

6. J. Ma, F. Yu, L. Zhou, L. Jin, M. Yang, J. Luan, Y. Tang, H. Fan, Z. Yuan and J. Chen, *ACS applied materials & interfaces*, 2012, **4**, 5749-5760.

7. L. Carson, C. Kelly-Brown, M. Stewart, A. Oki, G. Regisford, Z. Luo and V. I. Bakhmutov, *Mater Lett*, 2009, **63**, 617-620.

8. L. Qian and X. Yang, *Talanta*, 2006, **68**, 721-727.

9. J. Ma, Z. Zhu, B. Chen, M. Yang, H. Zhou, C. Li, F. Yu and J. Chen, *Journal of Materials Chemistry A*, 2013, **1**, 4662.

10. J. Ma, J. N. Wang and X. X. Wang, *Journal of Materials Chemistry*, 2009, **19**, 3033-3041.

11. X. Wang, R. Sun and C. Wang, *Colloids Surf. Physicochem. Eng. Aspects* 2014, **441**, 51-58.

12. G. Zhao, J. Li and X. Wang, *Chemical Engineering Journal*, 2011, **173**, 185-190.

13. M. A. Ahmad and R. Alrozi, *Chemical Engineering Journal*, 2011, **171**, 510-516.

14. X. Luo and L. Zhang, *Journal of hazardous materials*, 2009, **171**, 340-347.

15. H. Y. Zhu, R. Jiang, L. Xiao and W. Li, *Journal of hazardous materials*, 2010, **179**, 251-257.

16. L. Poon, S. Younus and L. D. Wilson, *Journal of colloid and interface science*, 2014, **420**, 136-144.

17. I. A. Tan, A. L. Ahmad and B. H. Hameed, *Journal of hazardous materials*, 2008, **154**, 337-346.

18. Y. Zhuang, F. Yu, J. Ma and J. H. Chen, *Rsc Adv*, 2015, **5**, 27964-27969.

19. Y. Zhuang, F. Yu, J. Ma and J. H. Chen, *New J Chem*, 2015, **39**, 3333-3336.

20. E. Erdem, N. Karapinar and R. Donat, *Journal of colloid and interface science*, 2004, **280**, 309-314.

21. S. S. Tahir and N. Rauf, *Chemosphere*, 2006, **63**, 1842-1848.

22. F. A. Bertoni, A. C. Medeot, J. C. Gonzalez, L. F. Sala and S. E. Bellu, *Journal of colloid and interface science*, 2015, **446**, 122-132.

23. D. K. Mahmoud, M. A. M. Salleh, W. A. W. A. Karim, A. Idris and Z. Z. Abidin, *Chemical Engineering Journal*, 2012, **181-182**, 449-457.

24. L. Obeid, A. Bee, D. Talbot, S. Ben Jaafar, V. Dupuis, S. Abramson, V. Cabuil and M. Welschbillig, *Journal of colloid and interface science*, 2013, **410**, 52-58.

25. W. H. Cheung, Y. S. Szeto and G. McKay, *Bioresource technology*, 2007, **98**, 2897-2904.

26. W. S. W. Ngah and M. A. K. M. Hanafiah, *Biochemical Engineering Journal*, 2008, **39**, 521–530.

27. Y. Safa and H. N. Bhatti, *Desalination*, 2011, **272**, 313-322.

28. Y. C. Chang and D. H. Chen, *Macromolecular bioscience*, 2005, **5**, 254-261.

29. S. Maghsoodloo, B. Noroozi, A. K. Haghi and G. A. Sorial, *Journal of hazardous materials*, 2011, **191**, 380-387.

30. H.-Y. Zhu, R. Jiang and L. Xiao, *Applied Clay Science*, 2010, **48**, 522-526.

31. O. Aksakal and H. Ucun, *Journal of hazardous materials*, 2010, **181**, 666-672.

32. M. Zhang, B. Ren, Y. Wang and C. Zhao, *Spectrochim Acta A Mol Biomol Spectrosc*, 2013, **101**, 191-195.

33. M. Zhang, D. Yang, B. Ren and D. Wang, *J Fluoresc*, 2013, **23**, 761-766.

34. L. Zhou, J. Jin, Z. Liu, X. Liang and C. Shang, *Journal of hazardous materials*, 2011, **185**, 1045-1052.

35. M. S. Chiou and H. Y. Li, *Chemosphere*, 2003, **50**, 1095-1105.

36. Y. Zhao, F. Tong, X. Gu, C. Gu, X. Wang and Y. Zhang, *Sci. Total. Environ.*, 2014, **470-471**, 19-25.

Graphicial abstract

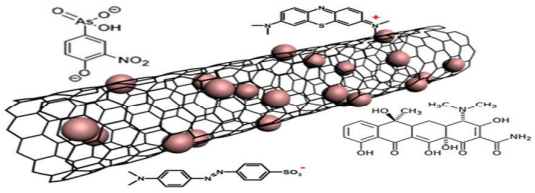

Adsorption properties of four organic pollutants on the carbon nanotubes/C@Fe/chitosan nanocomposite was studied.